

## **General Disclaimer**

### **One or more of the Following Statements may affect this Document**

- This document has been reproduced from the best copy furnished by the organizational source. It is being released in the interest of making available as much information as possible.
- This document may contain data, which exceeds the sheet parameters. It was furnished in this condition by the organizational source and is the best copy available.
- This document may contain tone-on-tone or color graphs, charts and/or pictures, which have been reproduced in black and white.
- This document is paginated as submitted by the original source.
- Portions of this document are not fully legible due to the historical nature of some of the material. However, it is the best reproduction available from the original submission.

Report on;

*1562*  
NASA Grant 1562

for Research Entitled:

"Effects of High Energy Radiation on the Mechanical Properties  
of Epoxy/Graphite Fiber Reinforced Composites"

Covering the period January 1, 1984 - December 31, 1984

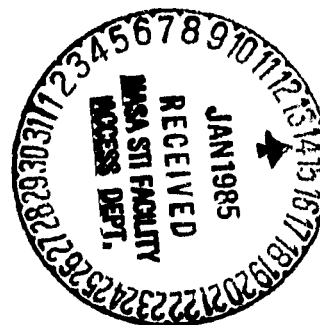
(NASA-CR-174314) EFFECTS OF HIGH ENERGY  
RADIATION ON THE MECHANICAL PROPERTIES OF  
EPOXY-GRAPHITE FIBER REINFORCED COMPOSITES  
Research Report, 1 Jan. - 31 Dec. 1984  
(North Carolina State Univ.) 58 p

N85-17047

Unclas  
G3/24 11502

Co-Principal Investigators

R.E. Fornes - Physics Department  
R.D. Gilbert - Textile Chemistry  
Department  
J.D. Memory - Physics Department



- I. Introduction
- II. Radiation Effects on Mechanical Properties of Composites and TGDDM/DDS Epoxy.
  - 1) Unirradiated Samples
  - 2) Irradiated Samples --
- III. Dynamical Mechanical Evaluation of TGDDM/DDS Epoxy and Graphite Fiber/Epoxy Composites.
- IV. Surface Analysis
  - 1) Sample Preparation
  - 2) Contact Angle Measurements
  - 3) ESCA and IR
  - 4) Discussion
- V. Electron Spin Resonance Spectroscopy Studies
  - 1) Sample Preparation
  - 2) ESR Studies of Graphite Fibers and Composites
  - 3) The Effect of Radiation Temperature on the ESR Lineshape
  - 4) Proposed Mechanism of Carbonyl Group Formation
- VI. Summary Discussion
- VII. Tables and Figures
- VIII. Appendices
  - A. Surface Energy Equations
  - B. Summary Listing of Publications, Presentations and Thesis
  - C. Abstracts of papers to be presented at the 1985 March Meeting High Polymer Section of the American Physical Society and one at the April Meeting of the American Chemical Society.

leveling of about  $2-5 \times 10^{19}$  radicals/g. Therefore, a graphite composite containing about 2/3 fiber mass would have its ESR signal dominated by the graphite. Indeed, as shown also in Figure 17, the signal of an unirradiated composite shows-essentially the same lineshape as that of fibers and the concentration is attributable to the fibers.

When fibers were irradiated (up to  $5 \times 10^3$  Mrad of 0.5 Mev electrons), no measurable increase in radical concentration was observed. Further, when composites were irradiated, the ESR spectra remained totally dominated by the signal from the graphite fibers (the estimated maximum height of the signal attributed to the epoxy is less than 1% of the maximum signal of that of the fibers). Whether the radicals on the fibers play a role in the decay and reaction of radicals in the matrix has not yet been determined.

### 3. The Effect of Radiation Temperature on the ESR Lineshape

Earlier we reported that the ESR signal of TGDDM/DDS epoxy irradiated ( $\gamma^{60}\text{Co}$ ) and maintained at liquid  $\text{N}_2$  (77°K) is a broad line with even broader shoulders that disappear within minutes at room temperature. The line remaining after a few minutes at room temperature is approximately symmetric and appears to be a singlet.

Shown in Figure 18 are the spectrum (I + II) of an epoxy irradiated and maintained  $\text{N}_2$  temperature, the spectrum (I) of the same sample after 30 minutes at room temperature, and the difference spectrum (II). Spectrum II shows that the signal of the short-lived radicals may be separated from that of the long-lived radicals and that the former signal appears to be either a sextet or an octet. Therefore, there may be as many as four different short-lived radicals present. We feel that the subtraction technique combined with measurements of lineshape changes with temperature will provide valuable information about the species of

radicals generated by ionizing radiation and the reaction mechanisms following radiation.

A difference was observed in the lineshapes of samples that were irradiated in air at room temperature and samples that were irradiated in liquid nitrogen and brought to room temperature (in air) for various times. There is a clearly observable asymmetry in the lineshapes of samples irradiated with either  $\gamma$  or electron irradiation in air while samples irradiated at ( $^{60}\text{Co}\gamma$ ) at  $77^\circ\text{K}$  then brought to room temperature appeared approximately symmetrical (see FIGURE 19). If the samples irradiated in air are left at room temperature for long times (Figure 20) the lineshape changes while the lineshape of the sample irradiated in liquid  $\text{N}_2$  remains approximately constant. This suggests that oxygen diffuses into the samples irradiated in air, reacts with the radicals and is responsible for the relatively narrow line observed in Figure 20.

In an attempt to eliminate the effect of oxygen, a sample of epoxy was prevacuumed for seven days at room temperature, sealed in Al foil, and then it was irradiated with  $^{60}\text{Co}\gamma$  at room temperature. Again, the lineshape appeared to be essentially identical to the sample which was left in air and irradiated (see Figure 21). This suggests that ~~elimination of oxygen was not achieved~~. Another explanation is that a different mechanism of radical decay occurs in samples irradiated at  $+77^\circ\text{K}$  and warmed to room temperature after radiation.

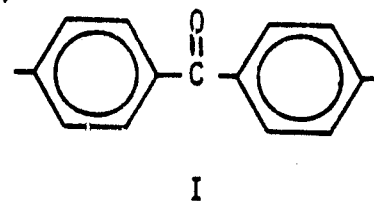
#### 4. Proposed Mechanism of Carbonyl Group Formation

There are two carbonyl peaks in the IR spectra of epoxy film after irradiation (Figure 15), viz, at  $1720\text{ cm}^{-1}$  and  $1660\text{ cm}^{-1}$ . The peak at  $1720\text{ cm}^{-1}$  is attributed to ketones or carboxylic acids and the peak at  $1660\text{ cm}^{-1}$  is due to an amide group.

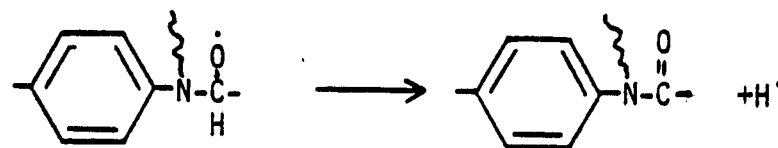
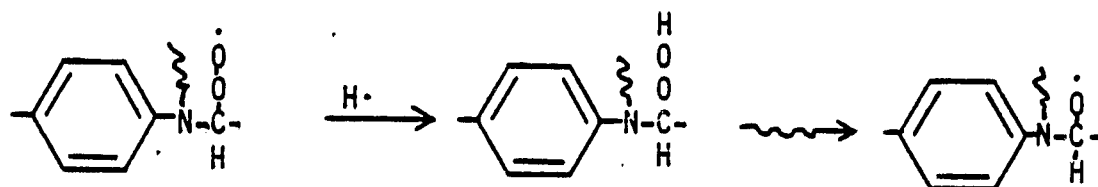
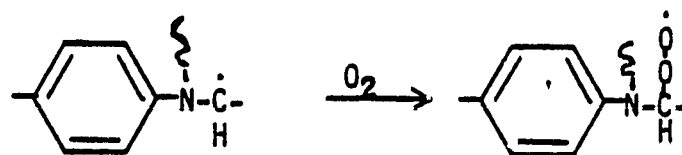
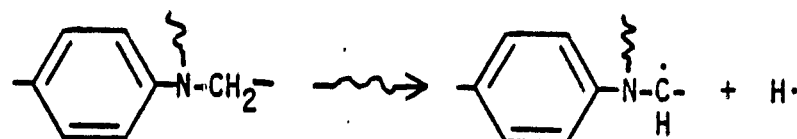
A possible mechanism for the carbonyl formation is as follows:



The oxidation of the methylene bridge of TGDDM seems to be very minor since the carbonyl peak at  $1720\text{ cm}^{-1}$  is at a much higher wavenumber than the expected for the carbonyl in I. Due to the highly conjugated structure of I, its carbonyl peak must appear at lower wavenumber than  $1715\text{ cm}^{-1}$  which is normal for a ketone.



#### Amide Formation



There are two possible sites for amide formation; DDS sites and TGDDM sites. The amide formation at the DDS site is less favorable than at TGDDM since the electron density at the nitrogen in DDS site is lower than that in TGDDM site.

Therefore the IR peak at  $1660\text{ cm}^{-1}$  is likely to be due to the amide formation in TGDDM. The increase of this peak was less than 15% with a 1,000 Mrad radiation dose.



## VI. Summary Discussion

The three point flexural stress and flexural modulus and the interlaminar shear stress (either in compression or tensile) data generally increase with radiation doses up to 10,000 Mrad (ignoring what is apparently a sample to sample variation, probably due to fabrication variation). The increase is particularly striking for the ILS strengths. The room temperature elastic modulus (measured on the Rheovibron) of the epoxy itself is reduced 50% after a 3100 Mrad dose. This indicates that considerable chain scission occurs in the epoxy on irradiation with high energy radiation particularly in the presence of oxygen.

ESR spectra of irradiated epoxy samples show radical species with at least two characteristic half-lives, one short-lived and one long-lived. The short-lived species are probably in regions of low crosslink density and due to their relatively high mobility either re-combine or react with oxygen. Either mode of decay could lead to additional crosslinking. The long-lived radical species are probably in areas of relatively high crosslink density, have lower mobilities which reduces their rate of recombination or crosslinking and their rate of reaction with oxygen due to their lower accessibility.

The evidence from surface studies, both contact angle and ESCA measurements, and infrared spectroscopy demonstrates convincingly that the radicals produced by irradiation react with oxygen. There are two possibilities that are suggested: (1) In spite of the fact the samples are evacuated prior to irradiation there is probably some residual oxygen in the samples, plus oxygen may have leaked into the system during irradiation. (2) Even if oxygen removal prior to irradiation was complete and the system was tight, reaction of the chain radicals with oxygen would occur rapidly on exposure of the samples to air because of the abundance of long-live radical species.

Chain scission and crosslinking occur concurrently when polymers are exposed to ionizing radiation. Usually one process dominates. The dynamic mechanical test suggests that chain scission dominates in the epoxy. The three-point bending tests and the ILS strength data indicate there is chain scission initially occurring in the epoxy matrix of the composite followed by crosslinking or interaction with the epoxy chain radicals with radicals on the surface of the graphite fibers, resulting in improved ILS strengths.

The ESR spectrum of unirradiated graphite fibers show there is an abundance of free radicals present (ca.  $10^{20}$ /g).

We have previously demonstrated that graphite fibers are not damaged by irradiation.

The problem that must be addressed is what would occur in a completely oxygen-free atmosphere, that is, in space? Undoubtedly, crosslinking would occur.



VII. Tables and Figures

Table I  
Summary of Mechanical Tests on Irradiated Composites

<u>Composite</u>	<u>Fiber Arrangement</u>	<u>Maximum Radiation Dose</u>	<u>Test*</u>	<u>Trend**</u>
T300/5208	Longitudinal	8,000 Mrad	TPB	I
T300/5208	Longitudinal	10,000 Mrad	ILS-TU	D
T300/5208	0/±45/0	10,000 Mrad	TPB	I
T300/5208	0/±45/0	10,000 Mrad	ILS-TU	D
T300/5208	90/±45/90	10,000 Mrad	TPB	I
T300/5208	90/±45/90	10,000 Mrad	ILS-TU	D
T300/5208	Transverse	10,000 Mrad	TPB	I
C6000/PMR15	Longitudinal	8,000 Mrad	TPB	I
C6000/PMR15	Transverse	10,000 Mrad	TPB	I
C6000/PMR15	Longitudinal	10,000 Mrad	ILS-TU	D
T300/5208	Longitudinal	9,000 Mrad	ILS-CS	I
T300/5208***	Longitudinal	9,000 Mrad	ILS-TU	I
T300/5208***	Longitudinal	9,000 Mrad	ILS-TS	I
T300/5209	Longitudinal	9,000 Mrad	ILS-CS	I
T300/5209***	Longitudinal	9,000 Mrad	ILS-TU	D
T300/5209***	Longitudinal	9,000 Mrad	ILS-TS	I
T300/5208	Longitudinal	10,000 Mrad	ILS-TU	I
T300/5208	0/±45/0	10,000 Mrad	ILS-TU	I
T300/5209	Longitudinal	7,500 Mrad	ILS-TU	I

\*ILS = Interlaminar shear

\*\*I = ILS increases with radiation dose

D = ILS decreases with radiation dose

\*\*\*Samples tested previously in ILS-CS mode

TU = Tensile, unsupported

TS = Tensile, supported

CS = Compressive, supported

Table II.  
Interlaminar Shear Stress by Compressive Force  
with a Side Support

<u>Sample</u>	<u>Radiation Dose (Mrad)</u>	<u>No. of Specimens</u>	<u>Shear Stress (Kg/cm<sup>2</sup>)</u>	<u>Standard Deviation</u>	<u>%CV</u>	<u>% change to control</u>
T300/5208	0	3	581	87.8	15.1	0
longitudinal	3000	5	654	48.3	7.3	+12.6
	6000	5	667	94.5	14.1	+14.8
	9000	5	784	51.6	6.5	+34.9
T300/5209	0	3	701	68.8	9.8	0
longitudinal	3000	5	765	158.3	20.7	+9.1
(notched after	6000	5	843	92.0	10.9	+20.3
irradiation)	9000	5	909	148.9	16.4	+29.7
T300/5209	6000	2	881	29.0	3.3	+25.7
longitudinal	9000	3	778	67.7	8.7	+11.0
(notched before irradiation)						

Table III.

Interlaminar Shear Stress by Tensile Force with  
a Side Support (samples loaded previously in  
ILS-CS mode)

<u>Sample</u>	<u>Radiation Dose (Mrad)</u>	<u>No. of Specimens</u>	<u>Shear Stress (Kg/cm<sup>2</sup>)</u>	<u>Standard Deviation</u>	<u>%CV</u>	<u>% change to control</u>
T300/5208	0	2	181.8	8.1	4.4	0
longitudinal	3000	5	186.6	28.2	15.1	+2.6
	6000	4	173.9	20.1	11.6	-4.3
	9000	4	215.0	18.1	8.4	+18.3
T300/5209	0	3	189.6	17.6	9.3	0
longitudinal	3000	4	205.2	21.9	10.7	+8.2
	6000	5	251.7	31.0	12.3	+32.8
	9000	5	234.0	38.7	16.6	+23.4

Table IV.  
Interlaminar Shear Stress by Tensile Force  
without a Side Support (samples loaded  
previously in ILS-GS mode)

<u>Sample</u>	<u>Radiation Dose (Mrad)</u>	<u>No. of Specimens</u>	<u>Shear Stress (Kg/cm<sup>2</sup>)</u>	<u>Standard Deviation</u>	<u>%CV</u>	<u>% change to control</u>
T300/5208	0	3	145.7	9.8	6.8	0
longitudinal	3000	5	133.7	25.5	19.1	-8.2
	6000	5	146.6	15.8	10.8	+0.6
	9000	5	174.5	18.1	10.3	+19.8
T300/5209	0	3	153.9	7.6	4.9	0
longitudinal	3000	5	171.9	25.3	14.7	+11.7
	6000	5	159.4	13.2	8.3	+0.4
	9000	5	123.1	17.3	14.1	-20.0

Table V.  
Interlaminar Shear Stress by Tensile Force  
without a Side Support

<u>Sample</u>	<u>Radiation Dose (MRAD)</u>	<u>No. of Specimens</u>	<u>Shear Stress (Kg/cm<sup>2</sup>)</u>	<u>Standard Deviation</u>	<u>%CV</u>	<u>% change to control</u>
T300/5208	0	9	154.1	20.8	13.5	0
longitudinal	2500	7	166.6	28.6	17.1	+8.1
	5000	10	176.2	28.0	15.9	+14.3
	7500	10	172.8	25.9	15.0	+12.1
	10000	8	157.1	16.3	10.3	+1.9
T300/5208	0	5	152.1	35.4	23.3	0
0/±45/0	2500	6	185.2	24.1	12.3	+21.8
	5000	9	193.0	27.2	14.1	+26.9
	7500	6	200.8	15.0	7.5	+32.0
	10000	7	246.1	21.9	8.9	+61.8
T300/5209	0	10	183.1	31.8	17.4	0
longitudinal	2500	10	215.5	21.3	9.9	+17.7
	7500	10	254.4	32.8	12.9	+38.9



Table VI.

Surface Tension Properties of Test Liquids at 20°C

<u>Test Liquid</u>	<u><math>\alpha_L</math></u>	<u><math>\beta_L</math></u>	<u><math>\gamma_{LA}^d</math></u>	<u><math>\gamma_{LA}^p</math></u>	<u><math>\gamma_{LA}</math></u>
Water	4.67	7.14	21.8	51.0	72.8
Formamide	5.68	5.10	32.3	26.0	58.3
Ethylene-glycol	5.41	4.35	29.3	19.0	48.3
1-Bromo-naphthalene	6.68	0.00	44.6	0.0	44.6
Tricresyl-phosphate	5.10	3.26	26.0	10.6	36.6
Hexadecane	5.25	0.00	27.6	0.0	27.6
Hexane	4.29	0.00	18.4	0.0	18.4

Note: $\alpha_L/\beta_L$ ; (dyne/cm)<sup>1/2</sup> $\gamma_{LA}$ ; dyne/cm

Table VII.

## Surface Energy of Irradiated Epoxy Films

<u>Dose</u> <u>Mrad</u>	$\gamma_{EA}^d$	$\gamma_{EA}^p$ <u>dyne/cm</u>	$\gamma_{EA}$	$\gamma_{EA}^p / \gamma_{EA}$
0	22.9	1.2	24.1	0.05
400	23.3	11.3	34.6	0.33
1,000	21.0	39.7	60.7	0.65
2,000	22.6	38.0	60.5	0.63
5,000	22.7	38.2	60.8	0.63
10,000	21.9	43.3	65.2	0.66

Table VIII.

## Surface Energy of Irradiated Graphite Fibers

<u>Dose</u> <u>Mrad</u>	<u><math>\gamma_{GA}^d</math></u>	<u><math>\gamma_{GA}^p</math></u> <u>dyne/cm</u>	<u><math>\gamma_{GA}</math></u>	<u><math>\gamma_{GA}^p / \gamma_{GA}</math></u>
0	21.2	34.5	55.7	0.62
1,000	20.1	42.3	62.3	0.68
5,000	20.0	42.6	62.6	0.68
10,000	19.3	44.6	64.0	0.70

Table IX.  
Relative Atomic Concentration of O and C

<u>Sample</u>	<u>O/C</u>	<u>O</u>	$\frac{O/C(\text{irradiated})}{O/C(\text{control})}$
Epoxy Film			
As cured	1	0.237*	1.37
10,000 Mrad	1	0.324*	
<u>Composite (fracture surface)</u>			
Control	1	0.237	1.50
10,000 Mrad	1	0.358	

\*Average value of two measurements for the same sample.

Table X.

Contact Angle of Composite Fracture Surfaces (degree)

	<u>Control</u>	<u>7,500 Mrad</u>
Fiber direction*	--	
Advancing	61.7	45.2
Receding	-	-
Lateral direction*		
Advancing	85	59
Receding	34	59
Outermost surface		
Advancing	88	54.3
Receding	83.3	53.6

\*Shear-fractured surface

Note:

Sample; T300/5209, Uniaxial

Liquid; H<sub>2</sub>O

T300/5208

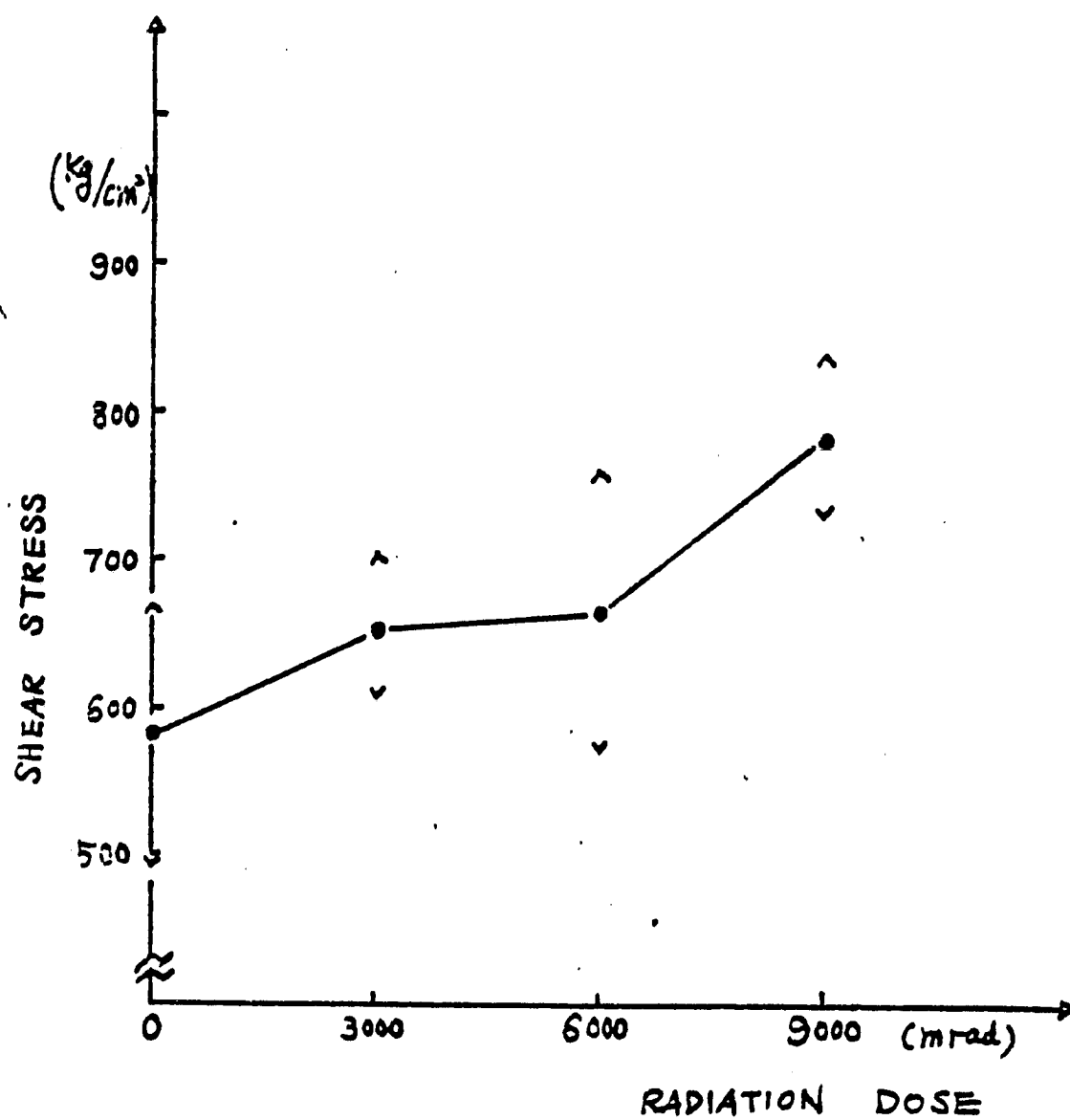


Fig. 1. Interlaminar Shear Stress versus radiation dose by compression using supporting fixture.

T 300/5209

$\hat{\odot}$  - notched after irradiation  
 $\hat{\boxplus}$  - notched before irradiation

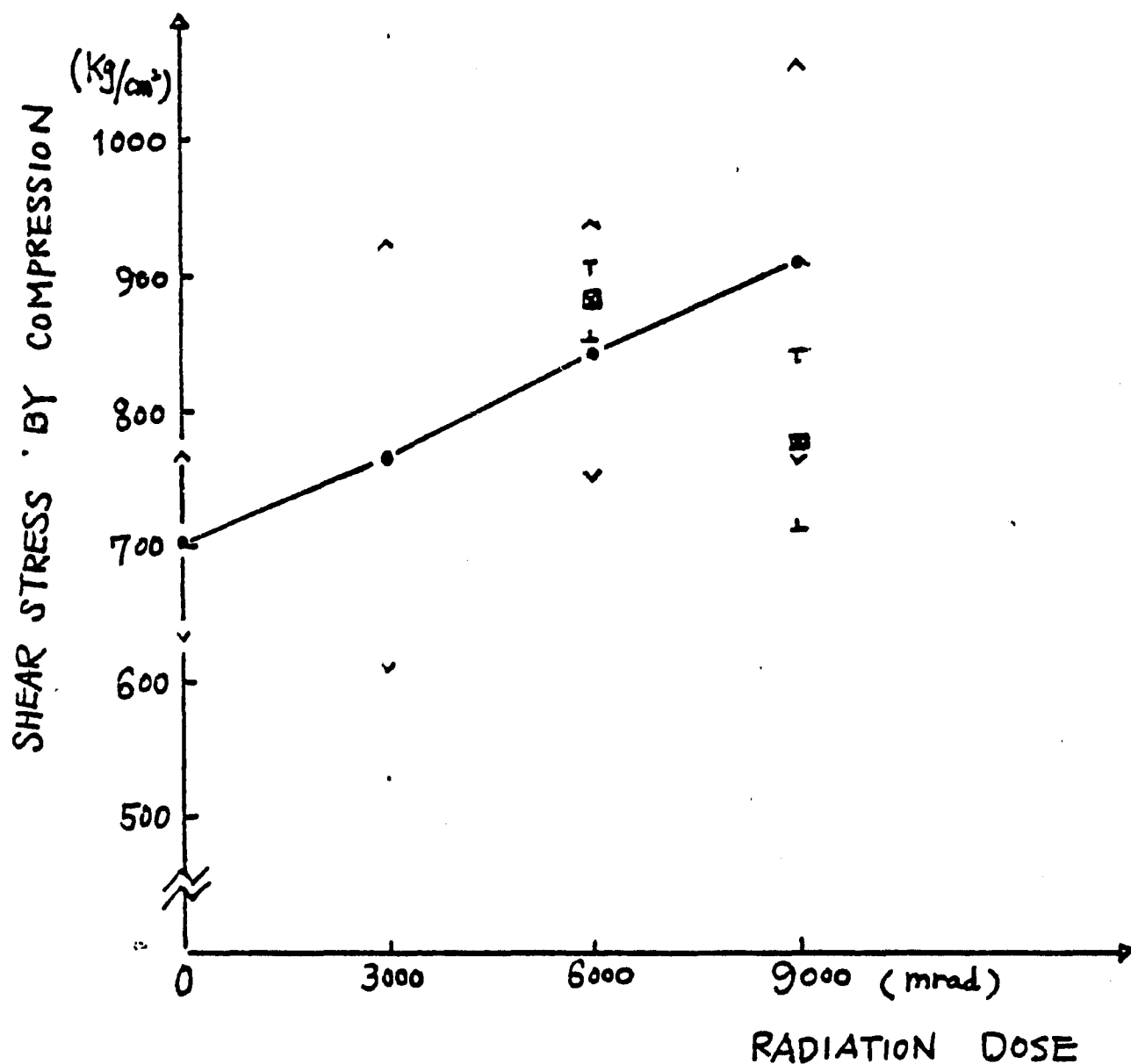


Fig. 2. Interlaminar Shear Stress versus radiation dose by compression using supporting fixture.

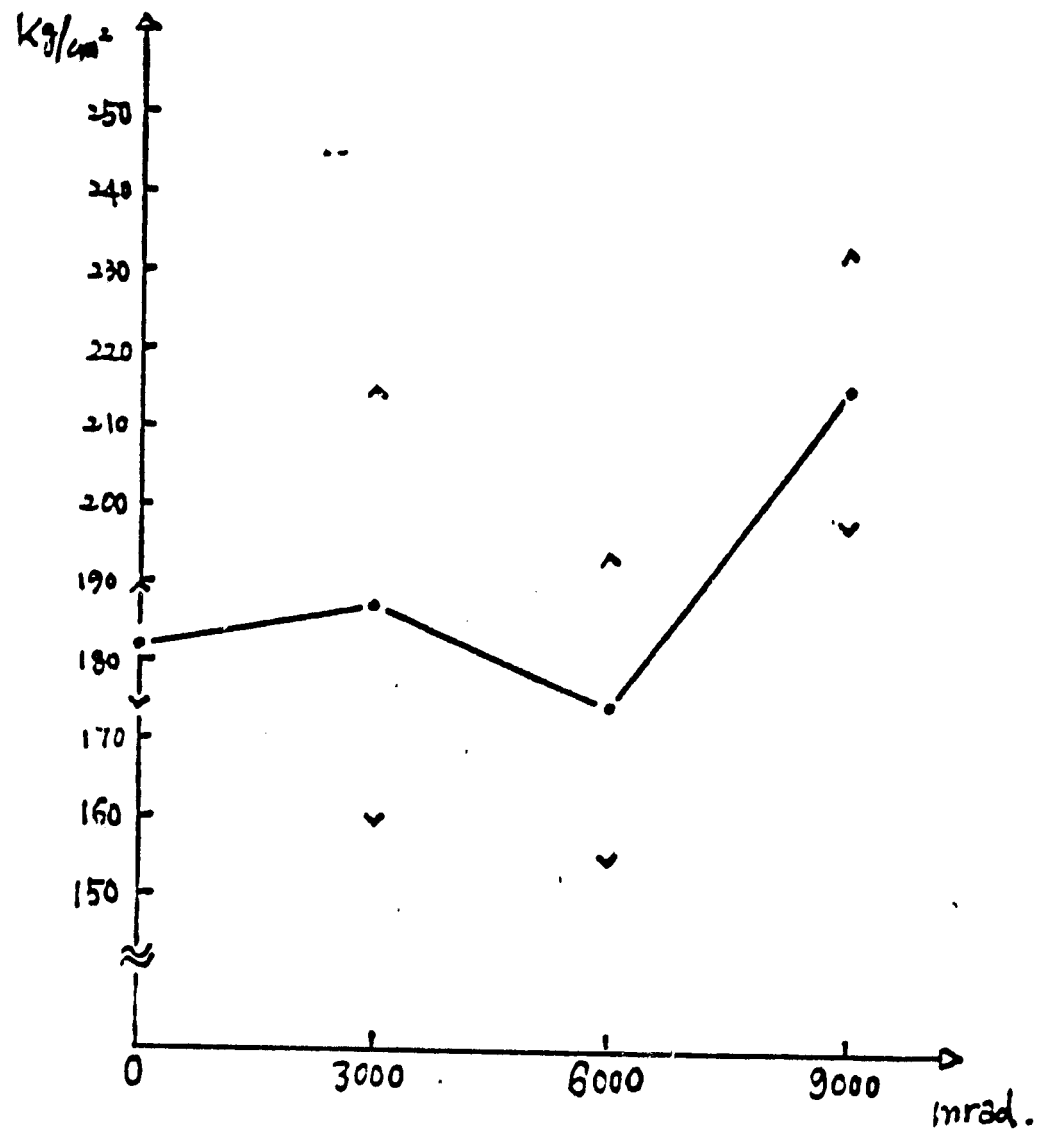


Fig. 3. Interlaminar shear stress versus Radiation dose in tension mode using supporting plate.



T 300/5209

⌘ - notched after irradiation  
⊖ - notched before irradiation

33.

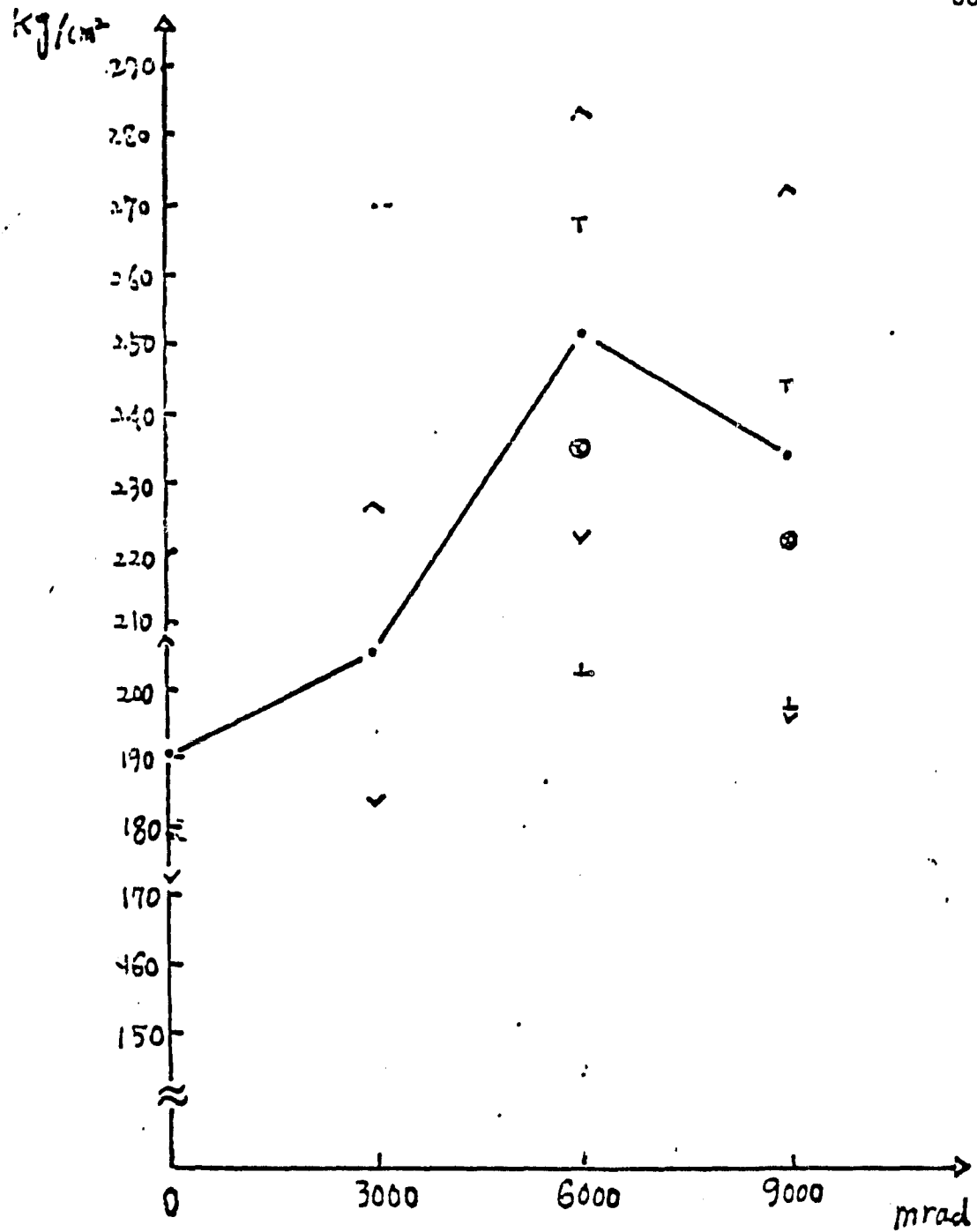


Fig. 4. Interlaminar Shear Stress versus Radiation dose in tension mode using supporting plate.

T300/5208

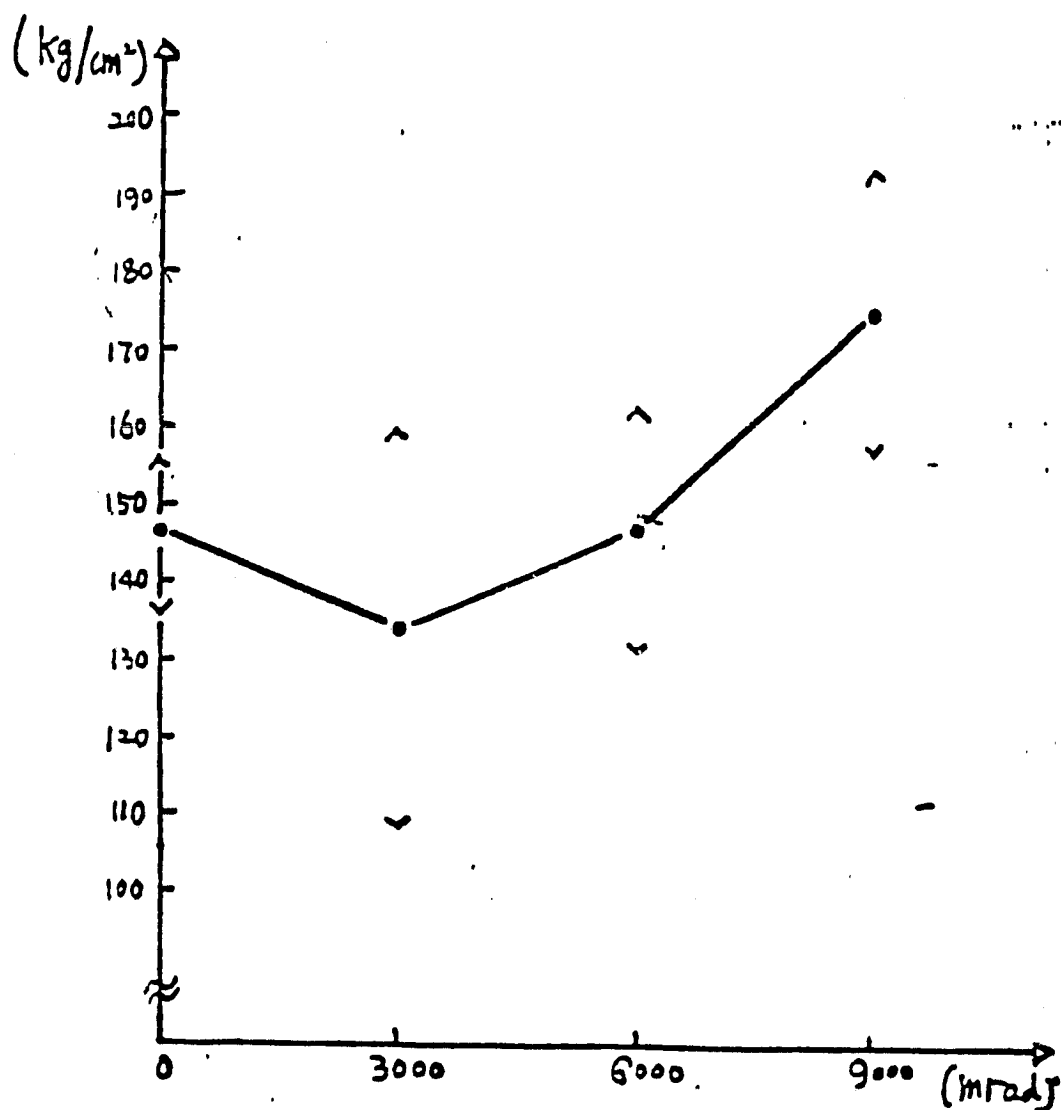


Fig. 5. Interlaminar Shear Stress versus Radiation dose in tension mode without using supporting plate.

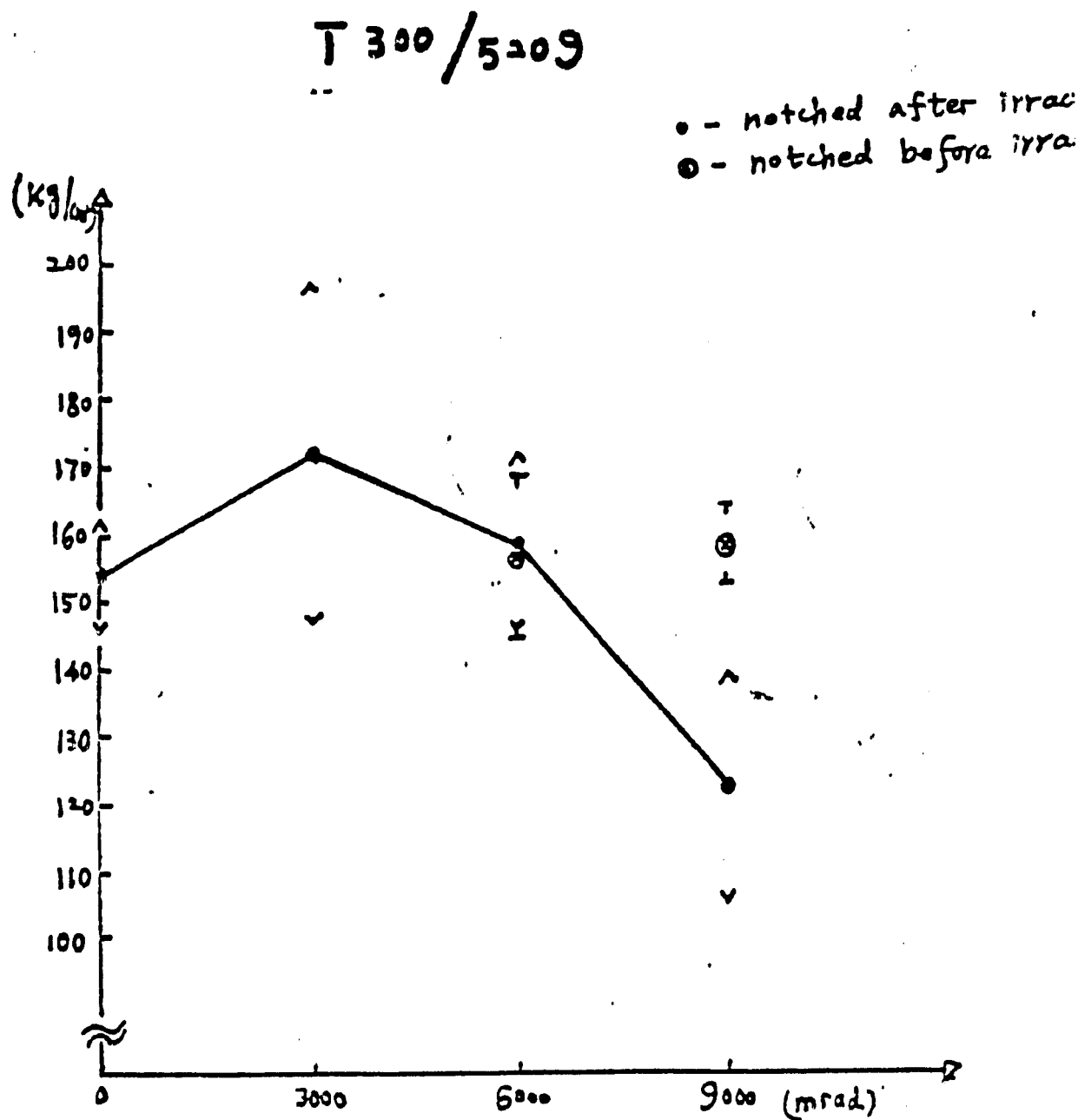


Fig. 6. Shear Stress versus Radiation dose in tension mode without using supporting plate.

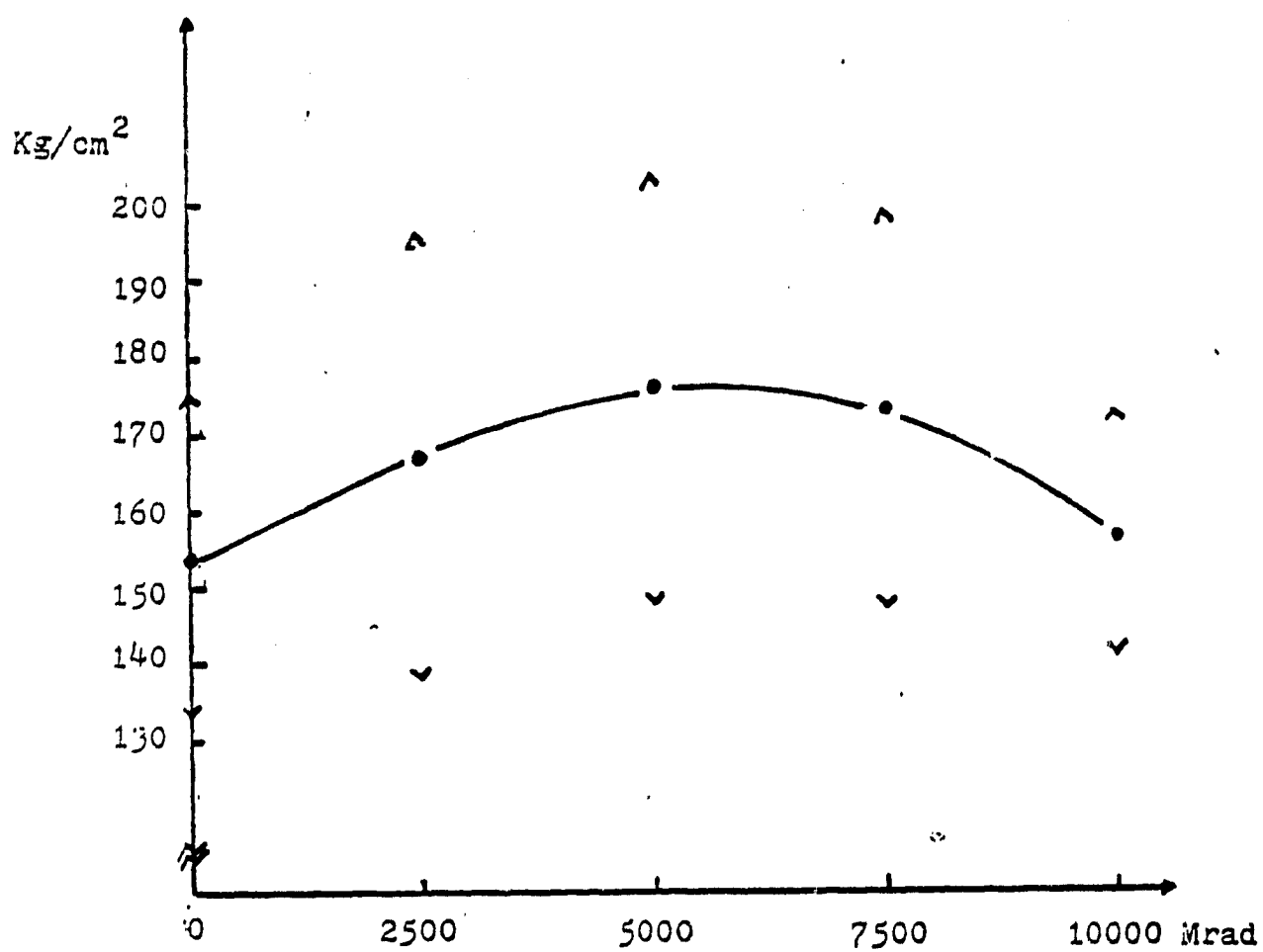


Fig. 7. Interlaminar Shear Stress in Tension mode without a supporting fixture for T300/5208 longitudinal samples.

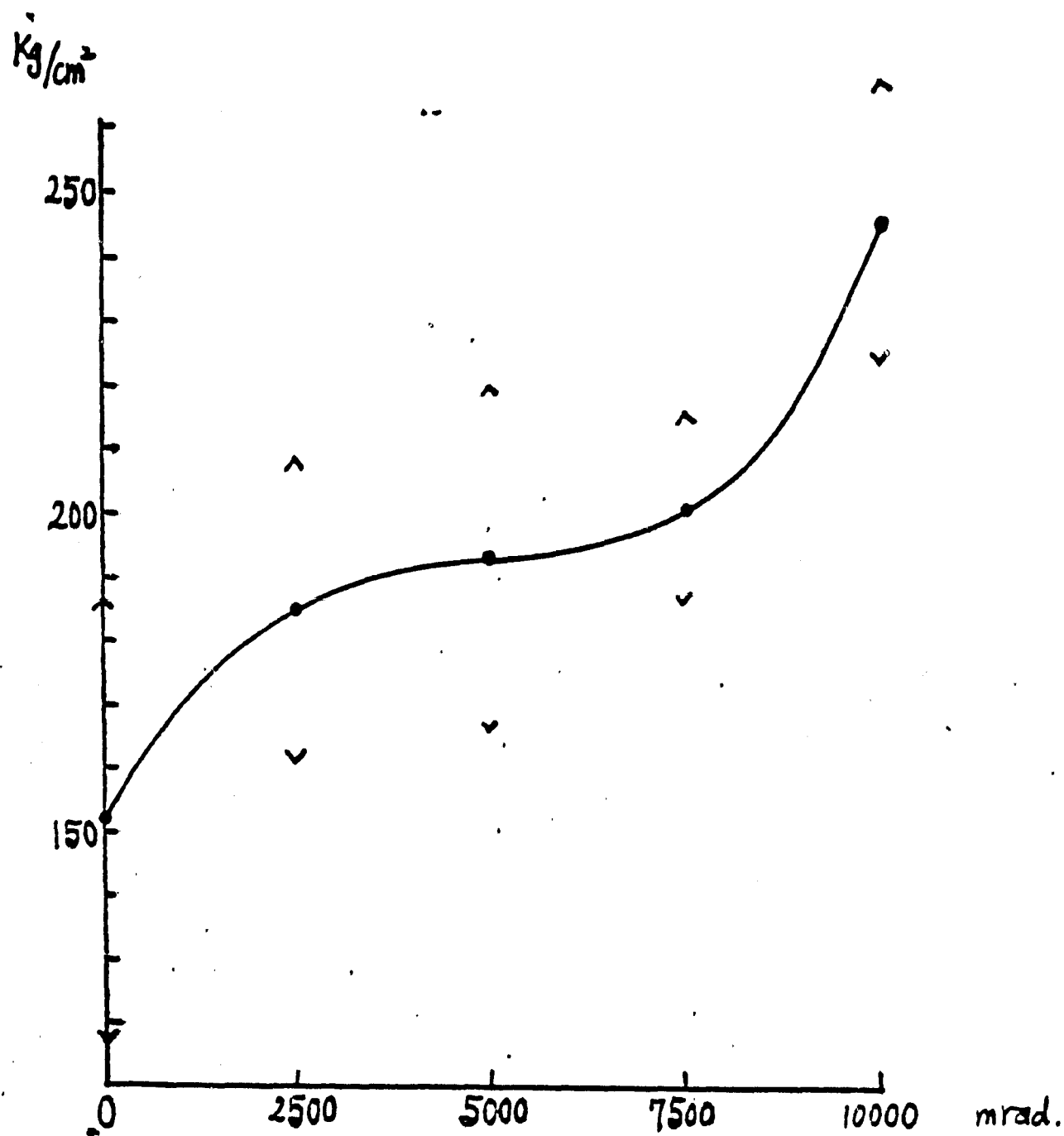


Fig. 8. I.L.S.S. in Tension mode w/o supporting fixture for T300/5208 0/± 45/0 ply.

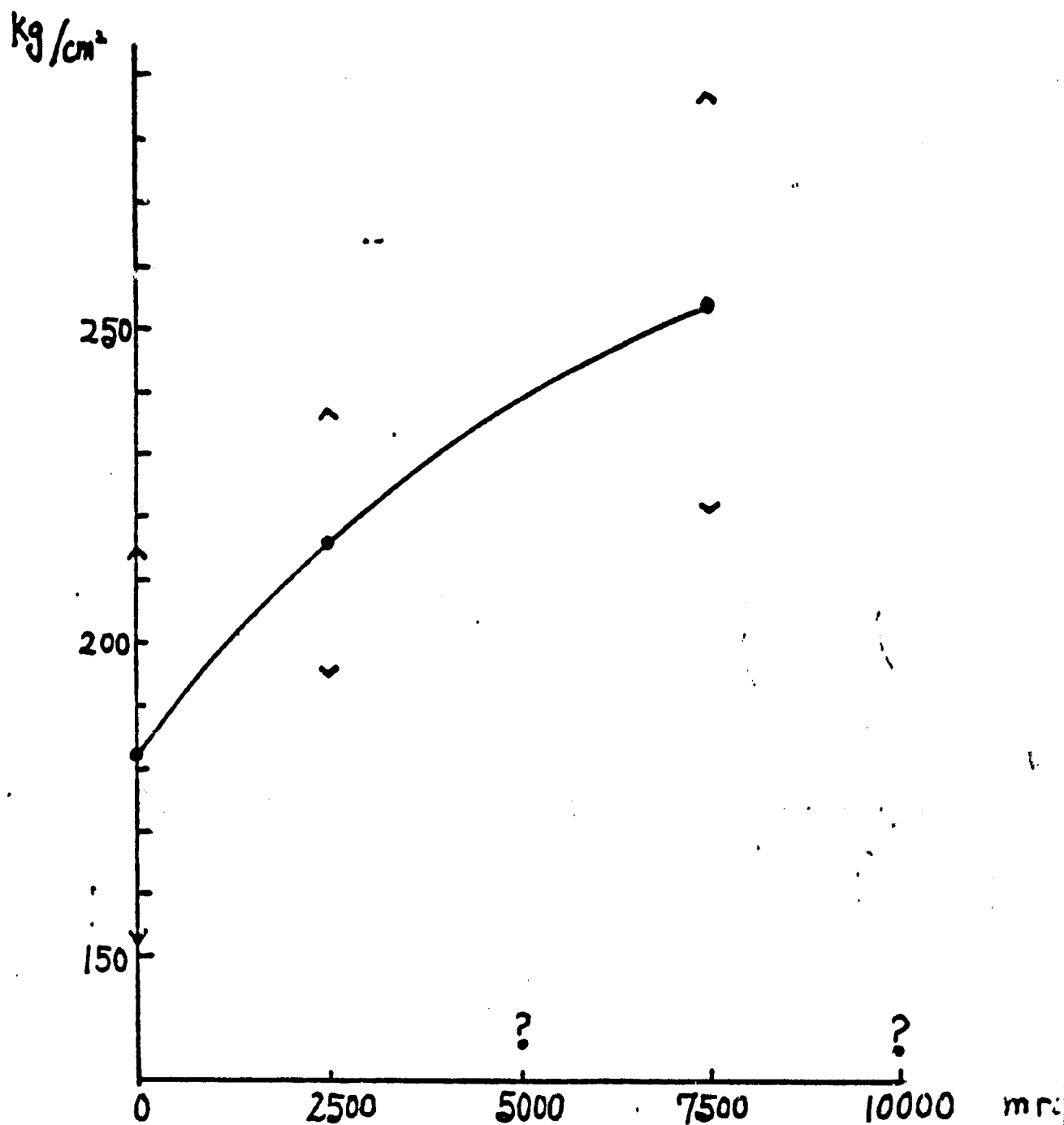
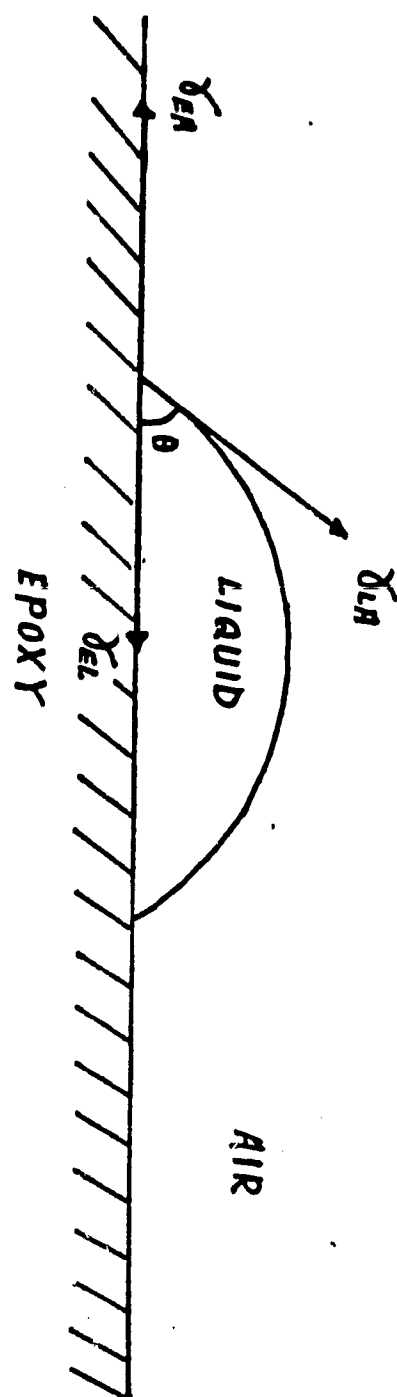
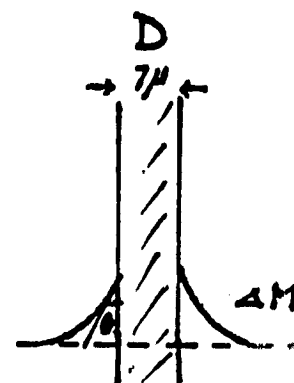
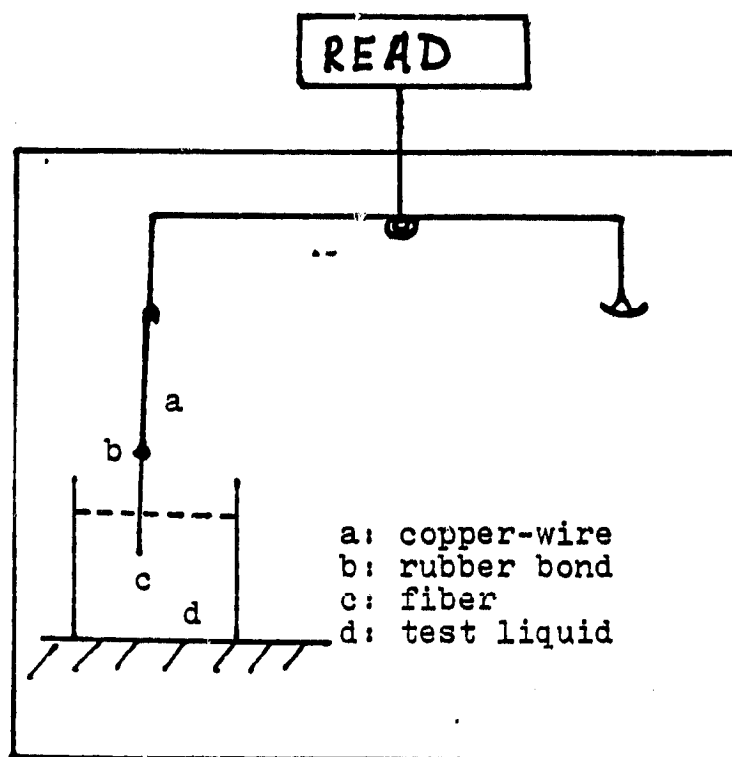


Fig. 9. I.L.S.S. in Tension Mode w/o supporting fixture for T300/5209 Uni-Dir.



$$\gamma_{EA} = \gamma_{EL} + \gamma_{LA} \cos \theta$$

FIG. 10 FORCES ACTING ON A LIQUID DROP RESTING ON THE EPOXY FILM.



$$\Delta M \cdot g = \pi D \gamma_{LA} \cos \theta$$

$$\cos \theta = \frac{\Delta M \cdot g}{\pi D \gamma_{LA}}$$

Fig. 11. A schematic diagram of Wilhelmy technique.

$\Delta M$ : weight difference before and after immersion of the fiber,  
 $g$ : 980.6 dyne/cm,  $D$ : diameter of the fiber,  $\gamma_{LA}$ : surface  
 tension of the test liquid.



## EPOXY (TGDDM-DDS)

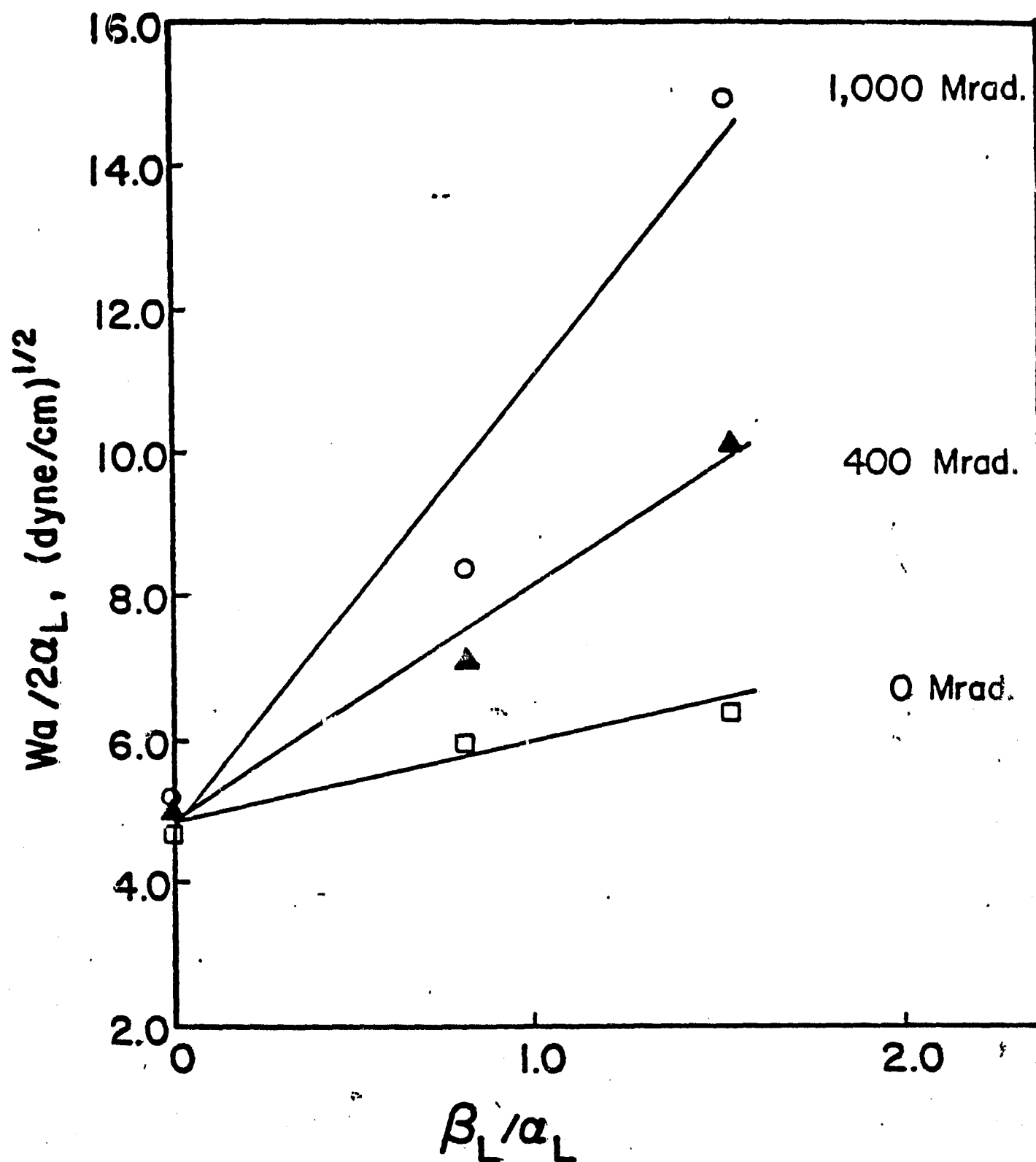


Figure 12. Plot of  $W_a/2\alpha_L$  against  $\beta_L/\alpha_L$  of Epoxy.

## GRAPHITE FIBER

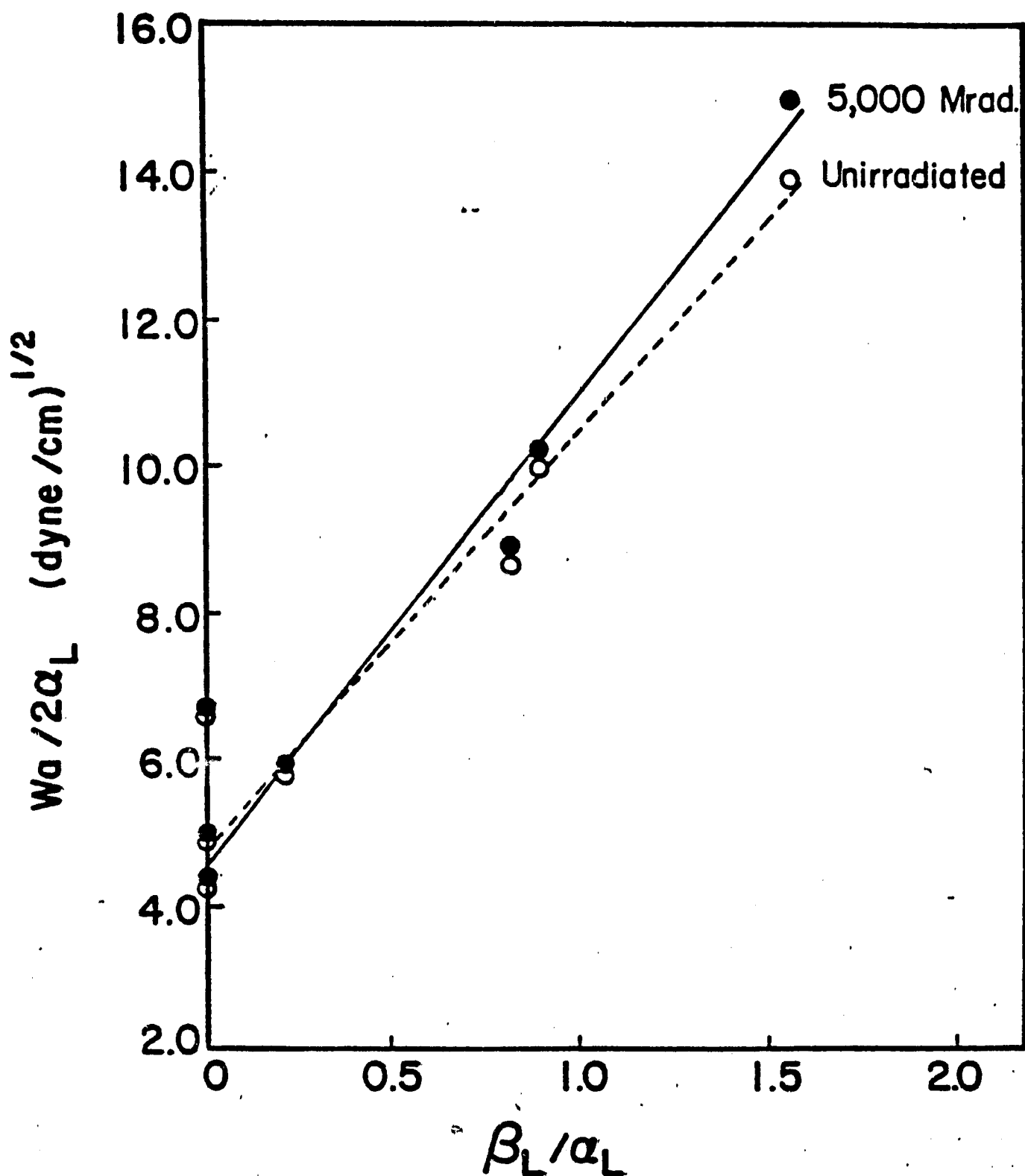


Figure 13. Plot of  $W/2\alpha_L$  against  $\beta_L/\alpha_L$  of graphite fiber.

# EPOXY (TGDDM - DDS)

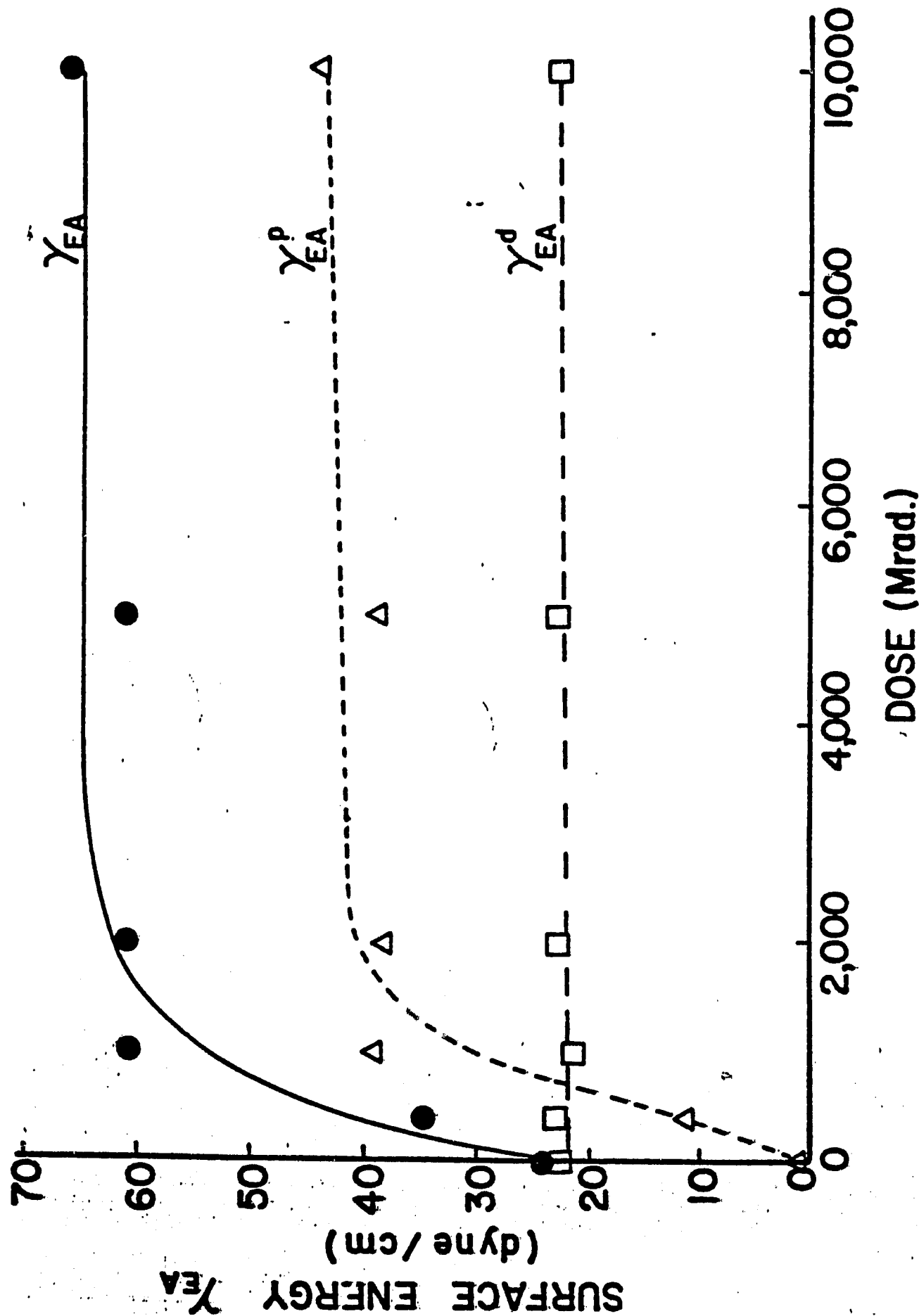
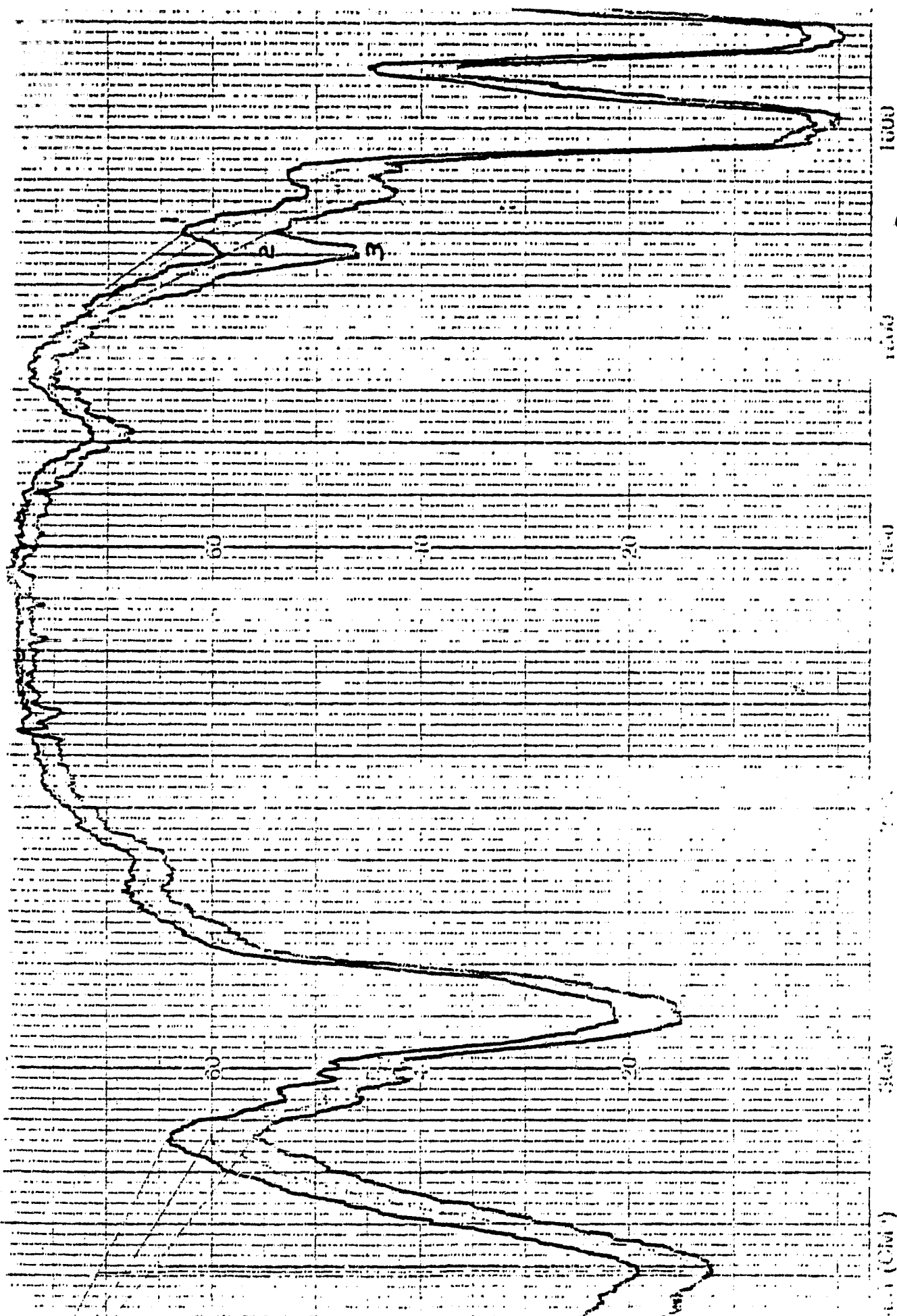


Figure 14. Plot of surface energy against irradiation dose of epoxy.



ORIGINAL PAGE IS  
OF POOR QUALITY

Fig. 15. Growth of carbonyl group ( $1720 \text{ cm}^{-1}$ ) with irradiation dose: 1- as cured, 2- 100 Mrad, 3- 1,000 Mrad. The sample was irradiated with 0.5 MeV electron beam and the doses indicated are cumulative ones.

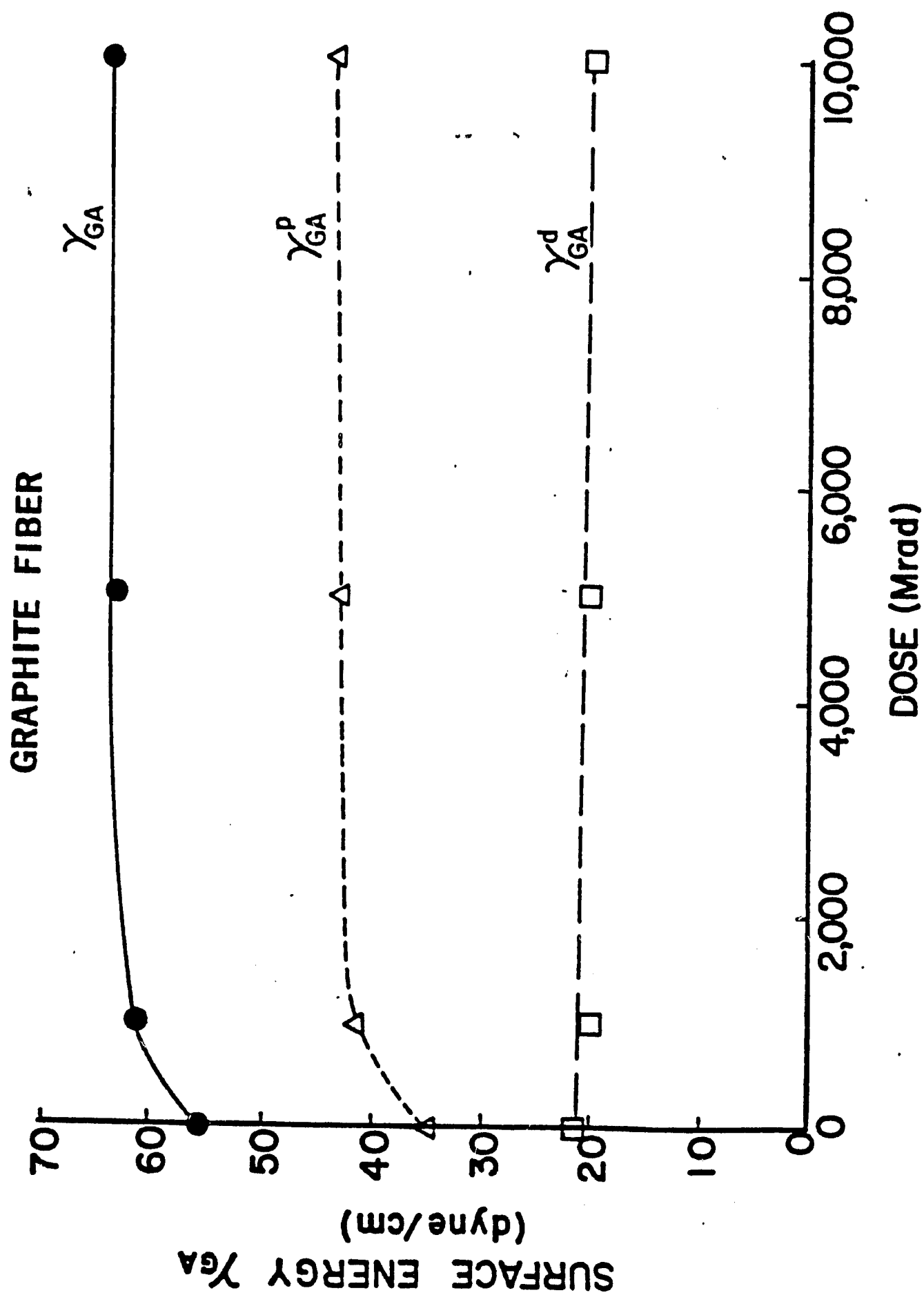


Figure 16. Plot of surface energy against irradiation dose of graphite fiber.

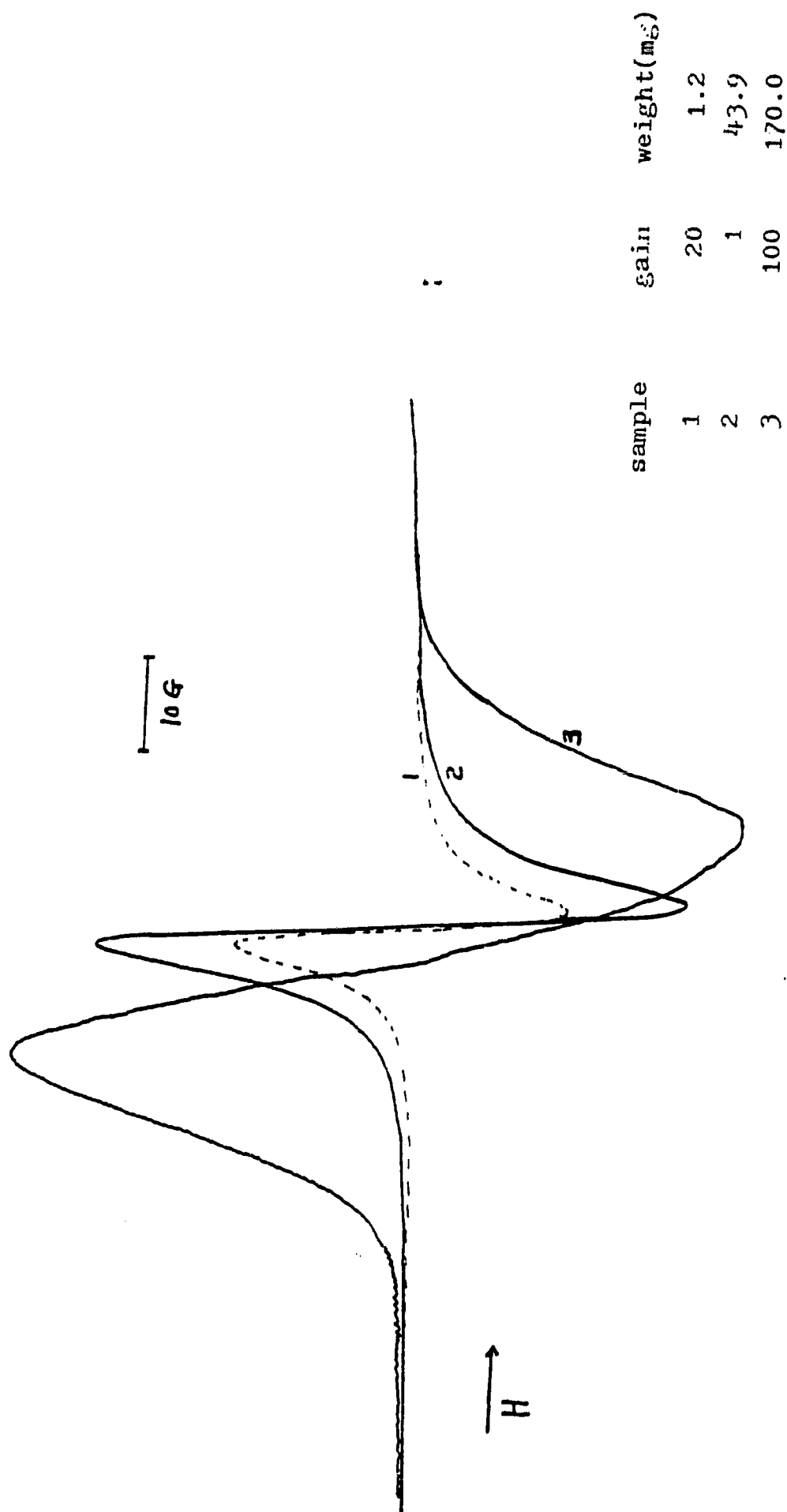


Fig. 17. Superposition of ESR spectra for : 1-graphite fiber(as-received, 2- composite (as-received ), 3- TGDDM-DDS epoxy ( 3 months after electron-irradiation, 5,000 Mrad ).

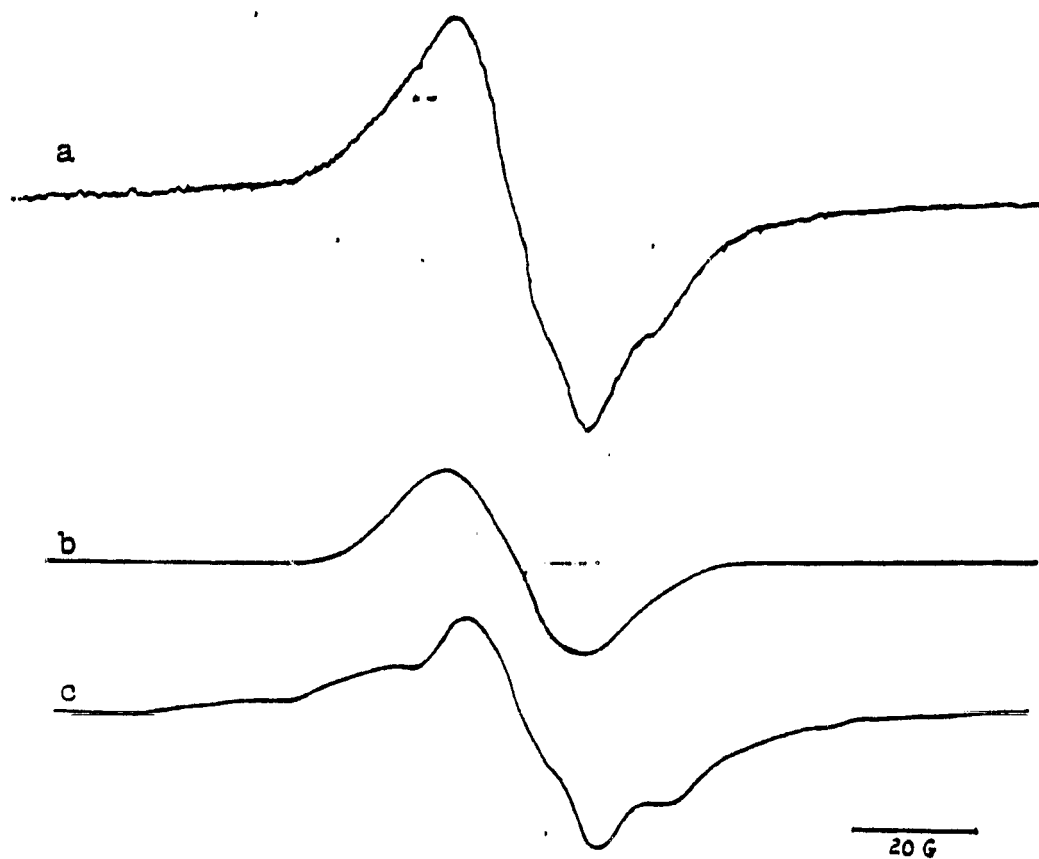


Fig. 18. ESR spectra of TGDDM-DDS epoxy irradiated with  $\gamma$ -radiation with a dose of 5 Mrad at liquid nitrogen temperature ( $-196^{\circ}\text{C}$ ): a. as-irradiated, b. after 200 min exposure to air at  $25^{\circ}\text{C}$ , c. spectra obtained by subtracting spectra b from spectra a.

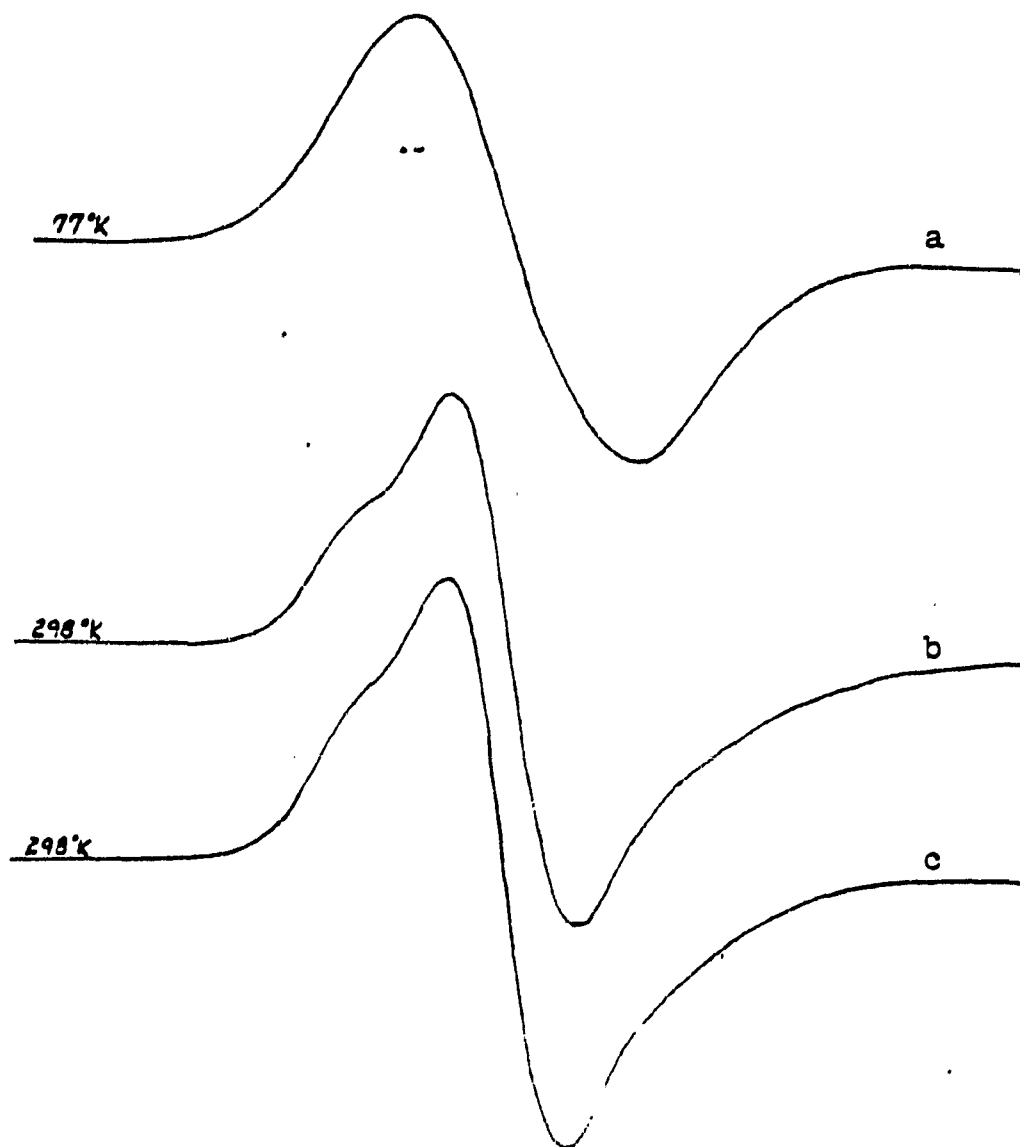


Fig. 19. ESR spectra of epoxy irradiated at various temperatures.

- a- 77°K,  $\gamma$ -radiation, 100 Mrad, 30 min. after irradiation, gain 1, mod. width 5.
- b- 298°K,  $\gamma$ -radiation, 100 Mrad, 30 min. after irradiation gain 5, mod. width 5.
- c- 298°K, electron beam (0.5 MeV), 160 Mrad, 5 min. after irradiation gain 1, mod. width 5.



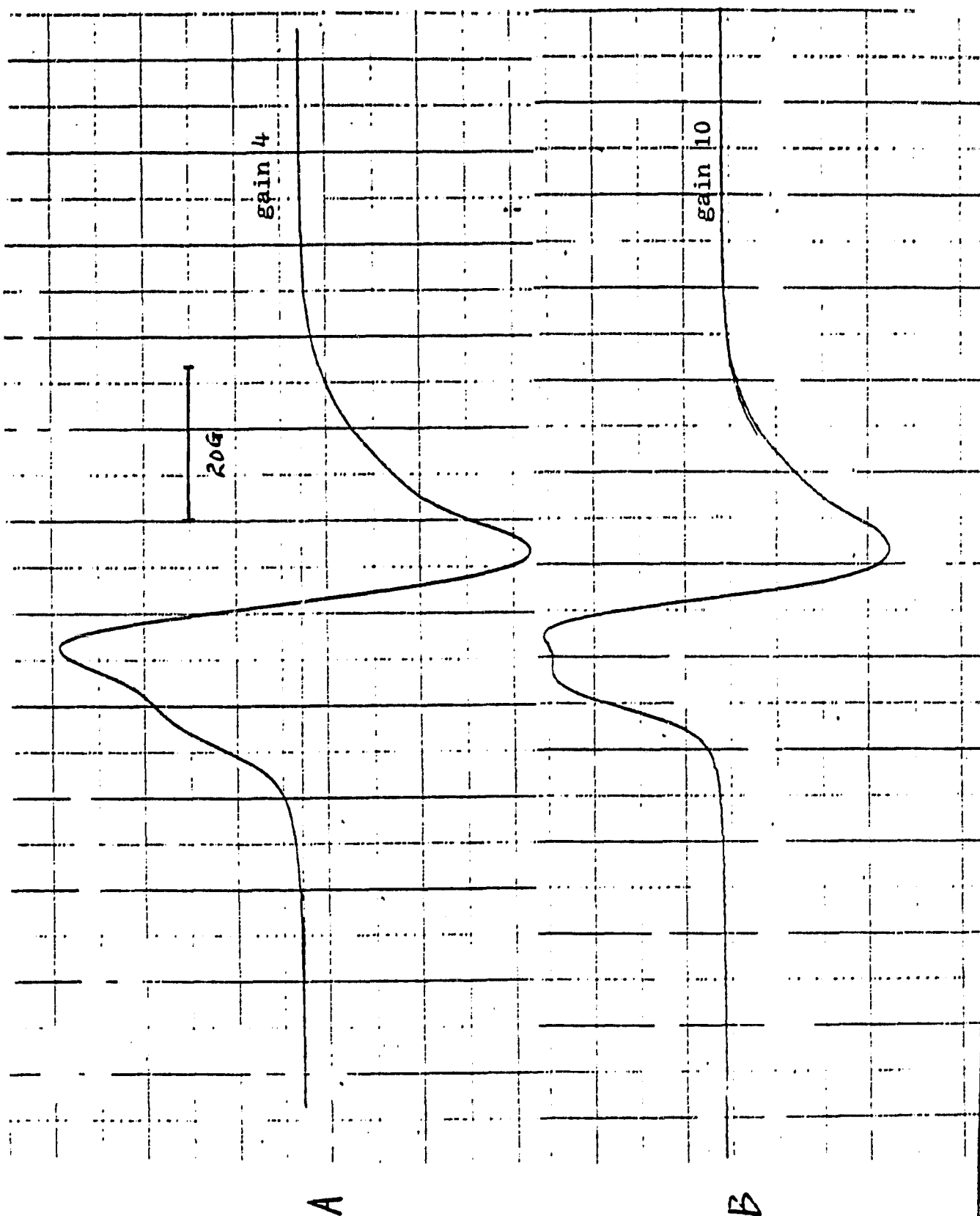


Fig. 20. ESR spectra of TGDDM-DDS epoxy irradiated with  $\gamma$ -ray at room temperature with a dose of 100 Mrad : A. as-irradiated, B. after 27 day exposure to air at 25°C.

ORIGINAL PAGE IS  
OF POOR QUALITY

ORIGINAL PAGE IS  
OF POOR QUALITY

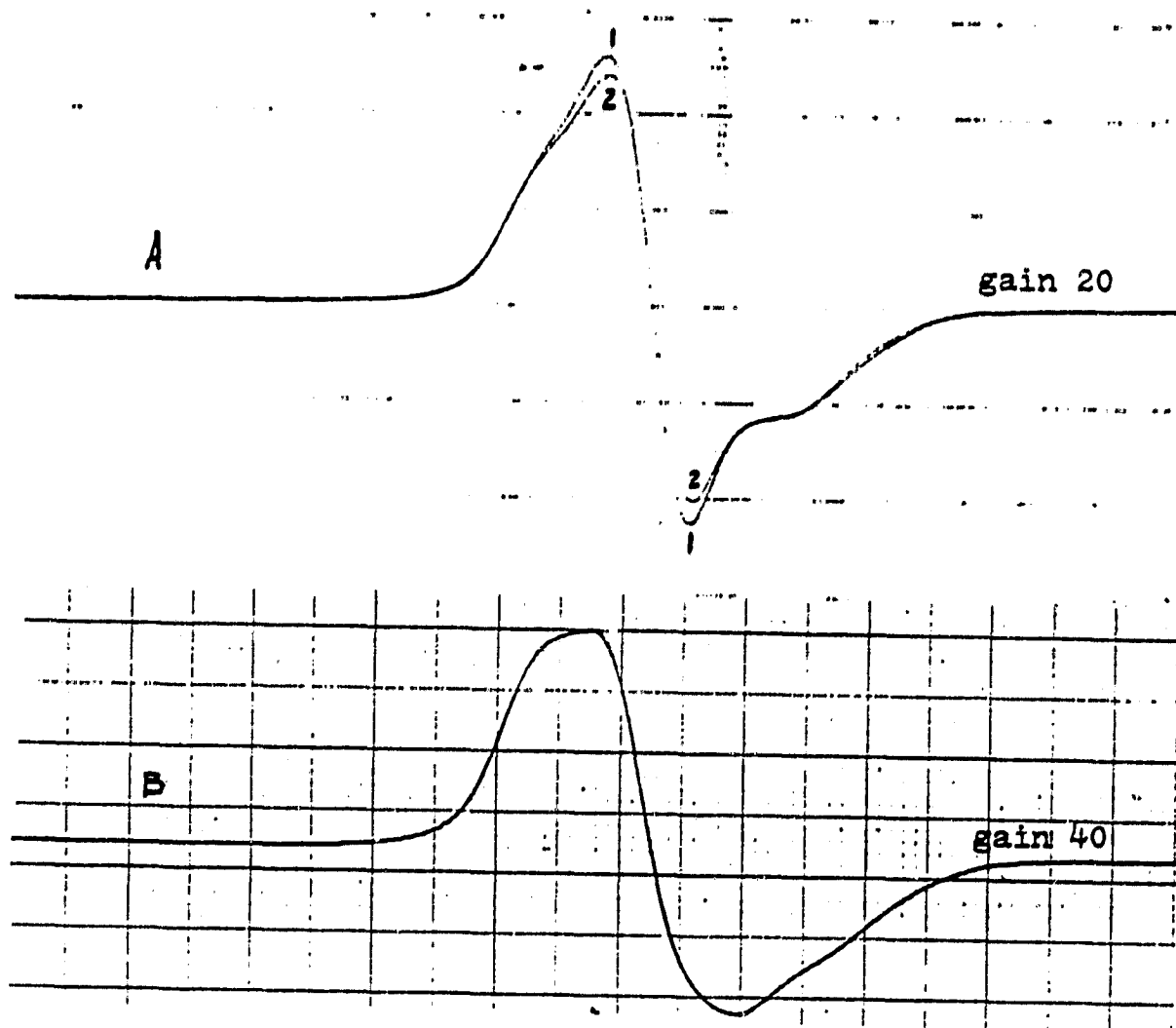


Fig. 21. ESR spectra of epoxy,  $\gamma$ -irradiated at room temperature with 800 Mrad :  
A1.as-irradiated in a vacuum-sealed glass tube, A2. as-irradiated in  
air, B. spectrum A1 after 90 day exposure to air at 25°C.

## VIII. Appendices

## Appendix A

$$\begin{aligned}\gamma_{LA} &= \gamma_{LA}^d + \gamma_{LA}^p = \alpha_L^2 + \beta_L^2 \\ \gamma_{EA} &= \gamma_{EA}^d + \gamma_{EA}^p = \alpha_E^2 + \beta_E^2\end{aligned}$$

$$W_a = \gamma_{LA} (1 + \cos \theta)$$

$$\begin{aligned}W_a &= 2[\alpha_L \alpha_E + \beta_L \beta_E] \\ &= W_a^d + W_a^p\end{aligned}$$

$$\frac{W_a}{2\alpha_L} = \alpha_E + \beta_E (\beta_L / \alpha_L)$$

$\gamma_{LA}$  = SURFACE ENERGY OF LIQUID

$\gamma_{LA}^d$  = DISPERSION COMPONENT OF SURFACE ENERGY OF LIQUID

$\gamma_{LA}^p$  = POLAR COMPONENT OF SURFACE ENERGY OF LIQUID

$\gamma_{EA}$  = SURFACE ENERGY OF EPOXY

$\gamma_{EA}^d$  = DISPERSION COMPONENT OF SURFACE ENERGY OF EPOXY

$\gamma_{EA}^p$  = POLAR COMPONENT OF SURFACE ENERGY OF EPOXY

$$\alpha_L = (\gamma_{LA}^d)^{1/2}$$

$$\beta_L = (\gamma_{LA}^p)^{1/2}$$

$$\alpha_E = (\gamma_{EA}^d)^{1/2}$$

$$\beta_E = (\gamma_{EA}^p)^{1/2}$$

$W_a$  = WORK OF ADHESION

## Appendix B

## Publications, Presentations and Theses Completed

## Publications:

1. R. E. Fornes, J. D. Memory and N. Naranong, "Effect of 1.33 MeV  $\gamma$  Radiation and 0.5 MeV Electrons on the Mechanical Properties of Graphite Fiber Reinforced Composites," J. Appl. Polym. Sci. **26**: 2061-2067 (1981).
2. R. E. Fornes, J. D. Memory, R. D. Gilbert and E. R. Long, Jr., "The Effects of Electron and Gamma Radiation on Epoxy-Based Materials," in Proceedings of Large Space Systems Technology (1981), NASA Conference Publication 2215, Part 3, Nov. 16-19, 1981, pp. 27-36.
3. K. Wolf, R. E. Fornes, J. D. Memory and R. D. Gilbert, "A Review of the Interfacial Phenomena in Graphite Fiber Composites," to be published in Chemistry and Physics of Carbon (Marcel Dekker, New York, Vol. 16 (1982)).
4. R. E. Fornes, J. D. Memory, N. Naranong, K. Wolf and W. C. Stuckey, "Radiation Effects on the Mechanical Properties of Graphite Fiber Reinforced Composites," Bull. Amer. Phys. Soc. **24**: 285 (1980).
5. N. Naranong, K. Wolf, J. D. Memory, R. D. Gilbert and R. E. Fornes, "Effects of Ionizing Radiation on the Mechanical and Morphological Properties of Graphite Fiber Reinforced Composites," Bull. Amer. Phys. Soc. **26**: 399 (1981).
6. K. Schaffer, R. D. Gilbert, J. D. Memory and R. E. Fornes, "Electron Spin Resonance Studies of Epoxy Samples Exposed to 1/2 MeV Electrons," Bull. Amer. Phys. Soc. **26**: 432 (1981).
7. M. Kent, K. Schaffer, J. D. Memory, R. D. Gilbert and R. E. Fornes, "Electron Spin Resonance Studies of Epoxy Exposed to  $\gamma^{60}\text{Co}$  Radiation," Bull. Amer. Phys. Soc. **27**: (3) p. 199 (1982).
8. N. Netravali, R. E. Fornes, R. D. Gilbert and J. D. Memory, "Thermal Analysis of Water Soaked Epoxy Resins," Bull. Amer. Phys. Soc. **27**: (3) 358-359 (1982).
9. K. Schaffer, R. E. Fornes, R. D. Gilbert and J. D. Memory, "ESR Study of a Cured Epoxy Resin Exposed to High-Energy Radiation," Polymer, **25**: 54-56 (1984).
10. A. N. Netravali, R. E. Fornes, R. D. Gilbert and J. D. Memory, "Investigation of Water and High Energy Radiation Interactions in an Epoxy," J. Appl. Polym. Sci., **29**: 311-318 (1984).

11. G. M. Kent, J. D. Memory, R. D. Gilbert and R. E. Fornes, "Variation in Radical Decay Rates in an Epoxy as a Function of Crosslinking Density," J. Appl. Polym. Sci., 28: 3301-3307 (1983).
12. R. E. Fornes, R. D. Gilbert and J. D. Memory, "Investigation of an Epoxy Interaction with H<sub>2</sub>O and High Energy Radiation," Journal of Research Communications, Spinal Publication, ARCSL-SP-83030  
Proceedings of the 1982 Scientific Conference on Chemical Defense, U.S. Army, Aberdeen, MD 21010 (1983).
13. M. Kent, K. Wolf, J. D. Memory, R. E. Fornes and R. D. Gilbert, "The Effect of 0.5 MeV Electron Radiation on the Crystallinity of Carbon Fibers in Composites," Carbon, 22: 103-104 (1984).
14. K. Wolf, R. E. Fornes, R. D. Gilbert and J. D. Memory, "Effects of 0.5 MeV Electrons in the Interlaminar and Flexural Strength Properties of Graphite Fiber Composites," J. Appl. Physics, 54: 5558-5561 (1983).
15. T. Wilson, R. D. Gilbert, J. D. Memory and R. E. Fornes, "Dynamic Mechanical Analysis of an Epoxy," Bull. Amer. Phys. Soc. 28: 392 (1983).
16. K. Wolf, J. D. Memory, R. D. Gilbert and R. E. Fornes, "Interlaminar Shear Properties of Irradiated Graphite Fiber Composites," Bull. Amer. Phys. Soc. 28: 549 (1983).
17. K. S. Seo, A. Netravali, R. D. Gilbert, J. D. Memory and R. E. Fornes, "Effects of High-Energy Radiation of Surface Energies of TGDDM/DDS Epoxy," Bull. Amer. Phys. Soc. 29: 410 (1984).
18. T. Wilson, J. D. Memory, R. D. Gilbert and R. E. Fornes, "Effects of 0.5 MeV Electron Radiation on Dynamic Mechanical Properties of TGDDM/DDS Epoxy," Bull. Amer. Phys. Soc. 29: 410 (1984).

#### Presentations:

R. E. Fornes, J. D. Memory and R. D. Gilbert, "Effects of Ionizing Radiation on the Mechanical and Structural Properties of Graphite Fiber Reinforced Composites," Gordon Research Conference on Fiber Science, July 1981.

Seminars presented on this work at Georgia Institute of Technology (May 1981), at the Polymer Group meeting, North Carolina Division, American Chemical Society, Raleigh, NC (January 1981), at the Jet Propulsion lab (1983, three seminars), at Lawrence Livermore Labs (1983, two seminars), at NASA Langley (1981, 1982, 1983) and at the U. Tennessee (1984), Fiber-Polymer Science Seminar at NCSU (1984), Nuclear Engineering Seminar at NCSU (1984), Honors Seminar at NCSU (1984) (see Bull. Amer. Phys. Soc. citations listed above).

Theses completed:

1. Naraporn Naranong, M.S. Thesis, "Effect of High Energy Radiation on Mechanical Properties of Graphite Reinforced Composites," (1980).
2. Kevin Schaffer, M.S. Thesis, "Characterization of a Cured Epoxy Resin Exposed to High Energy Radiation with Electron Spin Resonance," (1981).
3. George M. Kent, M.S. Thesis, "X-ray Diffraction and ESR Studies of the Effects of High Energy Radiation on Composite Materials," (1982).
4. Kay W. Wolf, Ph.D. Dissertation, "Effect of Ionizing Radiation on the Mechanical and Structural Properties of Graphite Fiber Reinforced Composites," (1982).